Materials Letters 198 (2017) 106–109

Contents lists available at ScienceDirect

Materials Letters

journal homepage: www.elsevier.com/locate/mlblue

Sulfur-doped, reduced graphene oxide nanoribbons for sodium-ion batteries

Young Soo Yun [a,*], Hyoung-Joon Jin [b,*]

[a] Department of Chemical Engineering, Kangwon National University, Samcheok 245-711, Republic of Korea
[b] Department of Polymer Science and Engineering, Inha University, Incheon 402-751, Republic of Korea

ARTICLE INFO

Article history:
Received 4 July 2016
Received in revised form 16 March 2017
Accepted 1 April 2017
Available online 4 April 2017

Keywords:
Graphene nanoribbon
Sulfur doping
Na-ion battery
Anode

ABSTRACT

This study focused on the effects of sulfur doping on the properties of thermally reduced graphene oxide nanoribbons (rGONRs) and their usage as anodes in Na-ion batteries. Sulfur-doped rGONRs (S-rGONRs) were fabricated by unzipping carbon nanotubes and thermally treating them with elemental sulfur. The prepared S-rGONRs showed a higher reversible capacity of 395 mAh g^{-1} than rGONRs, which have a capacity of 257 mAh g^{-1}. In addition, they exhibited high reversibility, a high rate capability of 20 A g^{-1}, and stable cyclic performance for over 4000 cycles.

1. Introduction

Nanostructured graphene derivatives (NGDs) have received considerable attention as a promising electrode material for energy storage [1–3] due to their high specific surface area, good electrical properties, and nanoscale properties such as their nanoelectronic [2] and nanoionic properties [3]. The charge storage mechanism of NGDs is made of a multitude of behaviors; while a perfect sp^2 hexagonal carbon structure cannot store charges by chemisorption, topological defect sites, such as pentagons, heptagons, vacancy defects, and edge defects, can act as redox hosts [4,5]. In addition, heteroatoms in the carbon structure can store charges reversibly [6]. Therefore, functionalized NGDs with a greater number of defects can potentially deliver much larger charges at faster rates.

Graphene nanoribbons (GNRs), which are one-dimensional carbon strips composed of an sp^2 hexagonal carbon structure, are one type of NGD [7]. GNRs have conventionally been prepared through a chemical route involving the unzipping of carbon nanotubes followed by reduction, since it is a relatively easy method for mass production [8]. During this process the surface of GNRs is highly oxidized and damaged by strong acidic reagents, leading to the introduction of numerous topological defects and oxygen functional groups [8]. While the electrical conductivity of GNRs prepared via this chemical route is greatly improved after reduction, considerable topological defects and heteroatoms remain in the structure of the GNRs. Chemically prepared GNRs are therefore distinct from other GNRs in terms of both their chemical structure and physical properties, and have been named graphene oxide nanoribbons (GONRs). GONRs have more redox-active sites than GNRs and are advantageous for scalable production. Moreover, the electrochemical performance of GONRs can be further increased by doping with additional redox-active heteroatoms [9]. Results from our previous research revealed that sulfur doping on graphene-based structures induced *n*-type doping defects, leading to enhancement of Li storage kinetics [10]. The sulfur atoms could additionally act as redox centers, thereby enhancing reversible capacities [10,11]. However, the effects of sulfur doping on charge storage of GONRs have not yet been reported. Furthermore, there is no information on the electrochemical properties of GONR-based anode materials for use in Na-ion batteries (NIBs).

For the above reasons, sulfur-doped and reduced GONRs (S-rGONRs) were fabricated and their electrochemical properties investigated in this study.

2. Experimental

GONRs were prepared according to a previously reported method [12], after which the freeze-dried GONRs were thermally treated with elemental sulfur (weight ratio of GONRs to sulfur was 1:1 *w*/*w*) at 600 °C in a tube furnace under a nitrogen atmosphere. A heating rate of 10 °C min^{-1} was applied and a holding time of 2 h used at the final temperature. The S-rGONRs were subsequently washed several times with ethanol and stored in a

* Corresponding authors.
E-mail addresses: ysyun@kangwon.ac.kr (Y. Soo Yun), hjjin@inha.ac.kr (H.-J. Jin).

http://dx.doi.org/10.1016/j.matlet.2017.04.001
0167-577X/

vacuum oven maintained at 25 °C. Control samples were prepared by following the same method, but omitting the treatment with elemental sulfur. Further specific methods, as well as materials and electrochemical characterization techniques are described in the supplementary information.

3. Results and discussion

The GONRs possessed a large number of oxygen functional groups with C—O and C=O bonding in the carbon structure, wherein the C/O ratio was 2.3 [Fig. 1(a)]. Simple heat treatment without elemental sulfur resulted in thermal reduction of the GONRs. In the X-ray photoelectron spectroscopy (XPS) C 1*s* spectrum of the reduced GONRs (rGONRs), C—O and C=O bonding peak intensities were considerably reduced, with a C/O ratio of 10.3 [Fig. 1(b)]. In contrast, heat treatment with elemental sulfur resulted in sulfur doping in addition to thermal reduction of the carbon structure. The XPS C 1*s* spectrum of S-rGONRs confirmed the presence of distinct C—S—C bonding centered at 284.5 eV, as well as C—C bonding centered at 284.4 eV and C—O bonding centered at 285.5 eV [Fig. 1(c)]. An interesting observation is the absence of the C(O)O bonding configuration in the S-rGONRs, suggesting that the edge sites of the S-rGONRs were fully functionalized by sulfur atoms. The XPS S 2*p* spectrum of S-rGONRs shows that sulfur atoms were mainly present in the form of S—C—S bond-

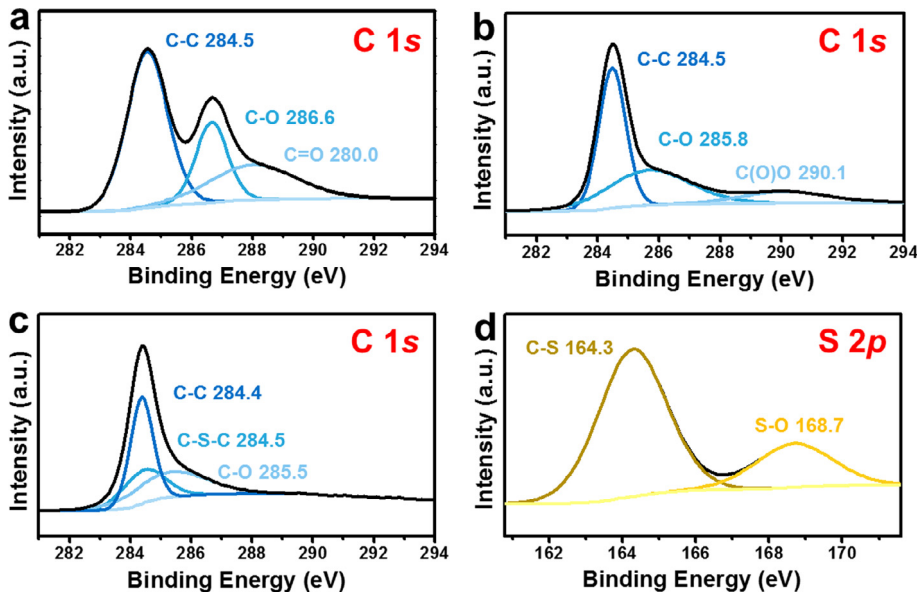

Fig. 1. XPS C 1s spectra of (a) GONRs, (b) rGONRs, and (c) S-rGONRs, as well as (d) XPS S 2*p* spectrum of S-rGONRs.

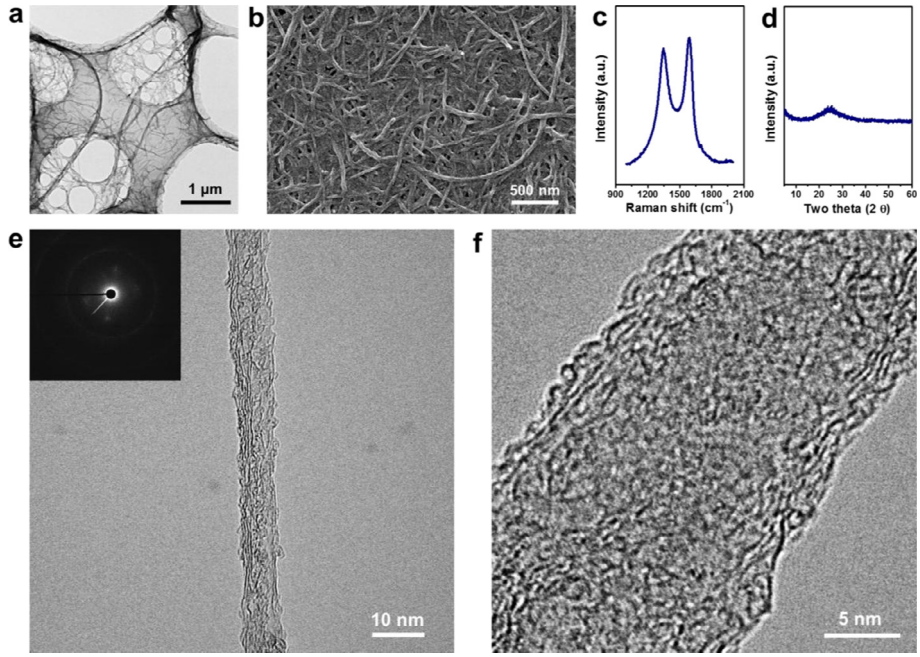

Fig. 2. (a) FE-TEM and (b) FE-SEM images of S-rGONRs. (c) Raman spectrum and (d) XRD pattern of S-rGONRs. (e), (f) High-resolution FE-TEM images of S-rGONRs at different magnification levels.

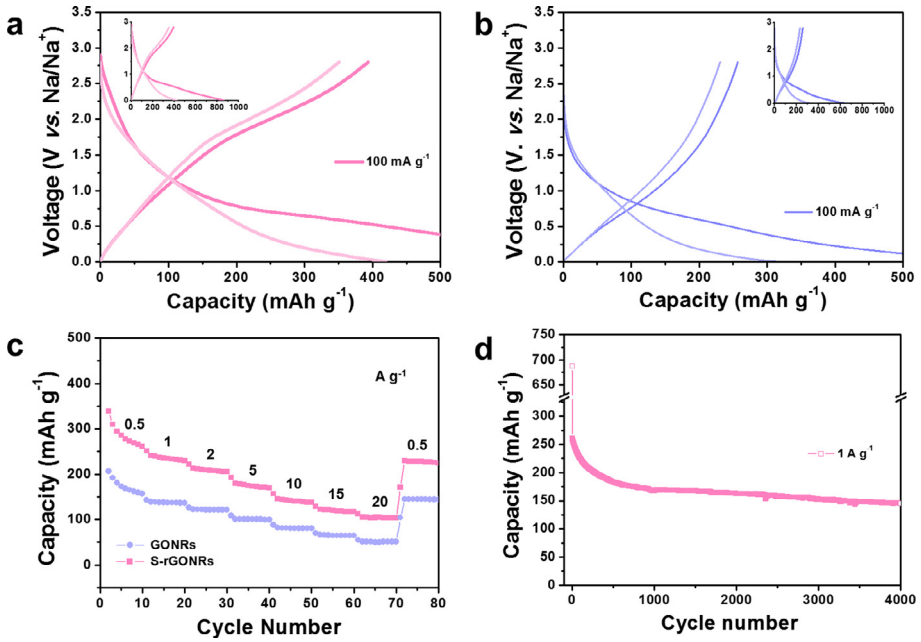

Fig. 3. Electrochemical performance of S-rGONRs over a voltage window of 0.01–2.7 V *vs.* Na/Na^+ in 1 M $NaPF_6$ dissolved in EC/DEC. Galvanostatic discharge/charge profiles of (a) S-rGONRs and (b) rGONRs at a current density of 100 mA g^{-1}. (c) Observed rate capabilities of S-rGONRs and rGONRs at current densities ranging from 0.5 to 20 A g^{-1}. (d) Cyclic performance of S-rGONRs at a current density of 1 A g^{-1} over 4000 cycles.

ing centered at 284.4 eV, with minor S—O bonding in the carbon structure [Fig. 1(d)]. The C/O ratio of the S-rGONRs was 6.4, much lower than that of the rGONRs, since the new S—O bonding in the S-rGONRs resulted in an increase in oxygen content. In addition, the C/S ratio was found to be 22.4.

The morphologies of the S-rGONRs are shown in Fig. 2 (a) and (b). S-rGONRs had a scale length of several micrometers and a thickness of ~20 nm, which corresponds to a high aspect ratio of >100. High-resolution field-emission transmission electron microscopy (FE-TEM) images of S-rGONRs revealed highly amorphized carbon structures without long-range carbon ordering, shown in Fig. 2(e) and (f). The selected area electron diffraction pattern, shown in the inset of Fig. 2(e), exhibits a very faint ring shape, confirming that the S-rGONRs had poor crystal structure. Specific microstructures of the samples were further characterized by Raman spectra and X-ray diffraction (XRD). The Raman spectra of the samples show distinct *D* and *G* bands centered at ~1344 and ~1581 cm^{-1}, respectively, as shown in Fig. 2(c). The I_D/I_G intensity ratio of the S-rGONRs was ~0.90, indicating that the hexagonal carbon structure was a few nanometers in size. The XRD pattern of S-rGONRs, shown in Fig. 2(d), contains a broad graphite (002) peak at 24.8°, indicating poor stacking ordering. The FE-TEM images, Raman spectrum, and XRD pattern taken together suggest that the S-rGONRs consisted of a disoriented assembly of numerous 2D hexagonal carbon nanocrystals.

The electrochemical performance of S-rGONRs is shown in Fig. 3. The galvanostatic discharge/charge profiles of S-rGONRs show a continuous decrease or increase in voltage without a plateau section, indicating the absence of equivalent Na-ion storage sites. Nevertheless, S-rGONRs exhibited a high reversible capacity of 395 mAh g^{-1} [Fig. 3(a)], much higher than those of reported carbon-based anode materials [13–18]. This high capacity of S-rGONRs could be induced mainly by pseudocapacitive behavior on the surface redox sites. The morphological and structural uniqueness of S-rGONRs, with many edge and topological defects and a large number of chalcogen heteroatoms, seem to be responsible for their high capacity. Moreover, the reversible capacity of S-rGONRs is also higher than that (257 mAh g^{-1}) of rGONRs [Fig. 3(b)], which can mainly be attributed to the doped sulfur atoms. Rate capabilities of S-rGONRs and rGONRs were tested at current densities from 0.5 to 20 A g^{-1}, as shown in Fig. 3(c). The reversible capacities of S-rGONRs gradually decreased with an increase in current density, and at a high current density of 20 A g^{-1}, a capacity of 104 mAh g^{-1} was maintained. In addition, when the current density returned to 0.5 A g^{-1} after 70 cycles, the S-rGONRs successfully regained their initial capacity, demonstrating very good reversibility. The rGONRs also exhibited good rate performance and reversibility; however, their capacities were much lower than those of S-rGONRs with respect to the overall current rate area. The cyclic stability of the S-rGONRs, tested over 4000 cycles at a current density of 1 A g^{-1}, was maintained overall, and after 4000 cycles a specific capacity of 145 mAh·g^{-1} was achieved.

4. Conclusion

To summarize, sulfur-doped reduced graphene oxide nanoribbons (S-rGONRs) were fabricated by unzipping carbon nanotubes and thermally treating them with elemental sulfur. S-rGONRs contained numerous oxygen and sulfur atoms and had C/O and C/S ratios of 6.4 and 22.4, respectively. The morphology of the S-rGONRs was characterized by a high aspect ratio of >100 and a fully amorphized carbon structure. The S-rGONRs further exhibited a high reversible capacity of 395 mAh g^{-1} at 100 mA g^{-1}; even at a high current density of 20 A g^{-1}, a capacity of 104 mAh·g^{-1} was maintained. Finally, stable cycle performance was maintained for over 4000 cycles.

Acknowledgments

This research was supported by Basic Science Research Program through the National Research Foundation of Korea (NRF) funded by the Ministry of Education (NRF-2016R1A2B4009601) and (NRF-2017R1C1B1004167).

Appendix A. Supplementary data

Supplementary data associated with this article can be found, in the online version, at http://dx.doi.org/10.1016/j.matlet.2017.04.001.

References

[1] T. Bhardwaj, A. Antic, B. Pavan, V. Barone, B.D. Fahlman, Enhanced electrochemical lithium storage by graphene nanoribbons, J. Am. Chem. Soc. 132 (2010) 12556–12558.

[2] W. Lu, C.M. Lieber, Nanoelectronics from the bottom up, Nat. Mater. 6 (2007) 841–850.

[3] J. Maier, Nanoionics: ion transport and electrochemical storage in confined systems, Nat. Mater. 4 (2005) 805–815.

[4] Y.S. Yun, K.Y. Park, B. Lee, S.Y. Cho, Y.U. Park, S.J. Hong, B.H. Kim, H. Gwon, H. Kim, S. Lee, Y.W. Park, H.J. Jin, K. Kang, Sodium-ion storage in pyroprotein-based carbon nanoplates, Adv. Mater. 27 (2015) 6914–6921.

[5] Y. Liu, V.I. Artyukhov, M. Liu, A.R. Harutyunyan, B.I. Yakobson, Feasibility of lithium storage on graphene and its derivatives, J. Phys. Chem. Lett. 4 (2013) 1737–1742.

[6] Y.S. Yun, D.H. Kim, S.J. Hong, M.H. Park, Y.W. Park, B.H. Kim, H.J. Jin, K. Kang, Microporous carbon nanosheets with redox-active heteroatoms for pseudocapacitive charge storage, Nanoscale 7 (2015) 15051–15058.

[7] J. Cai, P. Ruffieux, R. Jaafar, M. Bieri, T. Braun, S. Blankenburg, M. Mouth, A.P. Seitsonen, M. Saleh, X. Feng, K. Müllen, R. Fasel, Atomically precise bottom-up fabrication of graphene nanoribbons, Nature 466 (2010) 470–473.

[8] D.V. Kosynkin, A.L. Higginbotham, A. Sinitskii, J.R. Lomeda, A. Dimiev, B.K. Price, J.M. Tour, Longitudinal unzipping of carbon nanotubes to form graphene nanoribbons, Nature 458 (2009) 872–876.

[9] Y. Liu, X. Wang, Y. Dong, Z. Wang, Z. Zhao, J. Qiu, Nitrogen-doped graphene nanoribbons for high-performance lithium ion batteries, J. Mater. Chem. A 2 (2014) 16832–16835.

[10] Y.S. Yun, V.D. Le, H. Kim, S.J. Chang, S.J. Baek, S. Park, B.H. Kim, Y.H. Kim, K. Kang, H.J. Jin, Effects of sulfur doping on graphene-based nanosheets for use as anode materials in lithium-ion batteries, J. Power Sources 262 (2014) 79–85.

[11] Y. Yan, Y.X. Yin, S. Xin, Y.G. Guo, L.J. Wan, Ionothermal synthesis of sulfur-doped porous carbons hybridized with graphene as superior anode materials for lithium-ion batteries, Chem. Commun. 48 (2012) 10663–10665.

[12] M.Y. Song, Y.S. Yun, N.R. Kim, H.J. Jin, Dispersion stability of chemically reduced graphene oxide nanoribbons in organic solvents, RSC Adv. 6 (2016) 19389–19393.

[13] Y.X. Wang, S.L. Chou, H.K. Liu, S.X. Dou, Reduced graphene oxide with superior cycling stability and rate capability for sodium storage, Carbon 57 (2013) 202–208.

[14] K. Tang, L. Fu, R.J. White, L. Yu, M.M. Titirici, M. Antonietti, J. Maier, Hollow carbon nanospheres with superior rate capability for sodium-based batteries, Adv. Energy Mater. 2 (2012) 873–877.

[15] D. Li, L. Zhang, H. Chen, J. Wang, L.X. Ding, S. Wang, P.J. Ashman, H. Wang, Graphene-based nitrogen-doped carbon sandwich nanosheets: a new capacitive process controlled anode material for high-performance sodium-ion batteries, J. Mater. Chem. A 4 (2016) 8630–8635.

[16] X.U. Luo, C.H. Yang, Y.Y. Peng, N.W. Pu, M.D. Ger, C.T. Hsieh, J.K. Chang, Graphene, nanosheets, carbon nanotubes, graphite and activated carbon as anode materials for sodium-ion batteries, J. Mater. Chem. A 3 (2015) 10320–10326.

[17] Y.S. Yun, Y.U. Park, S.J. Chang, B.H. Kim, J. Choi, J. Wang, D. Zhang, P.V. Braun, H. J. Jin, K. Kang, Crumpled graphene paper for high power sodium battery anode, Carbon 99 (2016) 658–664.

[18] H. Liu, M. Jia, B. Cao, R. Chen, X. Lv, R. Tang, F. Wu, B. Xu, Nitrogen-doped carbon/graphene hybrid anode material for sodium ion batteries with excellent rate capability, J. Power Sources 319 (2016) 195–201.